# Microscopic Study of Wobbling Motions in Hf and Lu Nuclei

Yoshifumi R. Shimizu, Masayuki Matsuzaki*), and Kenichi Matsuyanagi**)
*Department of Physics, Graduate School of Sciences,*
*Kyushu University, Fukuoka 812-8581, Japan*
*) *Department of Physics, Fukuoka University of Education,*
*Munakata, Fukuoka 811-4192, Japan*
**) *Department of Physics, Graduate School of Sciences,*
*Kyoto University, Kyoto 606-8502, Japan*

**Abstract**

One of the most striking findings in the recent high-spin spectroscopy is the discovery of one-phonon, and possibly double-phonon, excitation of the nuclear wobbling rotational bands. In this talk, we first review the properties of observed wobbling motions, and discuss the failure and success of the possible interpretation in terms of the simple rotor model. Then, we further present results of our microscopic study in Hf and Lu nuclei by means of the theoretical framework, the cranked mean-field and the random phase approximation.

## 1 Introduction

In this talk we would like to discuss the nuclear wobbling motion. The wobbling motion is a spinning motion of asymmetric top, namely triaxial rigid-body. Quite recently, rotational bands associated with this motion have been identified in Lu nuclei[1)], and this discovery of the wobbling rotational bands is one of the most exciting topics in the nuclear spectroscopy. We must confess that we have been working on the wobbling motion for rather long period. In fact the talker(YRS)'s doctor thesis is somewhat related to it. So we are very regrettable that we have not been able to predict the possible existence of them in the Lu isotopes before the experiments.

The reason why the wobbling motion is so exciting is that it is related to a fundamental question: How does an atomic nucleus rotate as a *three-dimensional* object? Namely, the rotational motion is neither uniform, nor the conventional one where the axis of rotation coincides with one of principal axes. Here we would like to stress that most of the rotational bands, including the striking high-spin 2:1 superdeformed bands, are supposed to be based on the uniform rotation around the axis perpendicular to the symmetry-axis of deformation, so they are not genuine three-dimensional rotation. Since the existence of the wobbling motion requires the triaxial deformation, it also gives a rare chance to study the nuclear mean-field with triaxial deformation, which is very scarce near the ground state region.

Recently, another type of exotic rotations, other than the usual rotations around the perpendicular axis of axially symmetric nuclei, have been also reported; that is the "tilted axis rotation" or "magnetic rotation[2)]", which is conceptually different from the wobbling motion. The wobbling motion is non-uniform rotation and, just like the classical rigid body rotation, the angular momentum vector is not parallel to the rotational frequency vector, while the tilted axis rotation is an uniform rotation so that the two vectors are parallel with each other. The typical electromagnetic transitions associated with the wobbling excitations are electric quadrupole (E2), while the magnetic dipole (M1) transitions are very large in the tilted rotational bands. Another important difference is that the tilted rotational band appears as an isolated band (or a pair of bands in the case of recently proposed "chiral rotation/vibration"[3),4)]), while the wobbling motion manifest itself as a multi-rotational-band structure, reflecting that the complex rotational motions are composed of non-linear superposition of three rotations around three principal axes of triaxially deformed body.

The band structure associated with the wobbling motion is shown schematically in Fig. 1. The lowest band, namely the yrast band, corresponds to an uniform rotation around the axis of largest moment of inertia. One-phonon wobbling band is a rotational band with a quantized wobbling phonon being excited

on top of the yrast band, which leads to a fluctuating motion of the rotation axis with respect to the one in the yrast band. Two-phonon wobbling band corresponds to the band with two-wobbling quanta being excited on the yrast, and the amplitude of fluctuation of the rotation axis is getting larger. Three or more phonon bands are similar and based on multi-phonon excitations. The characteristic of this band structure is that relatively strong non-stretched E2 transitions connect the $n$-phonon and $(n-1)$-phonon bands: The horizontal bands are usual rotational sequences with strong stretched $\Delta I = \pm 2$ E2 transitions, while the vertical out-of-band transitions between, e.g., one-phonon to vacuum yrast band are $\Delta I = \pm 1$ E2 transitions, which are weaker than the horizontal ones but much stronger than the usual vibrational transitions. The energy of vertical excitation $\hbar\omega_{\rm w}$ is common in all the $(n-1)$-phonon to $n$-phonon excitations and E2 transitions between the $n$-phonon and $(n-2)$-phonon bands are prohibited in a harmonic approximation. This wobbling energy $\hbar\omega_{\rm w}$ is given by the well known formula[5] in terms of three moments of inertia around the principal axes of a rotating body, which is discussed more closely in the following sections.

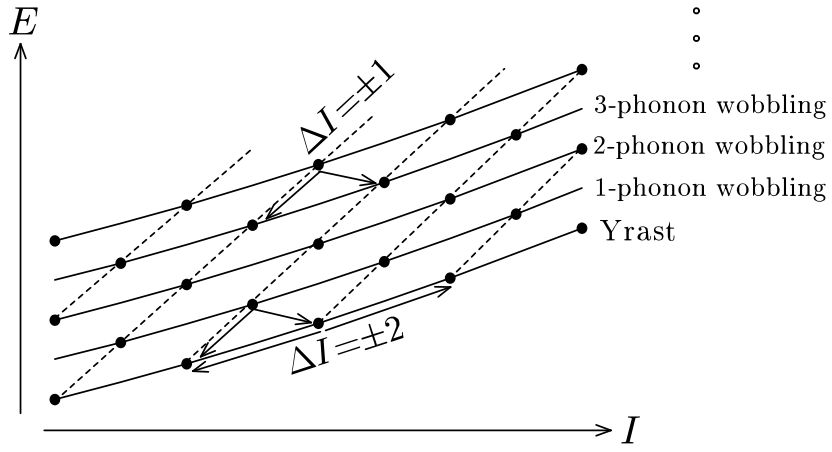


Figure 1: Schematic figure representing the multi-rotational-band structure of the wobbling motion.

## 2 Wobbling Motion: Observation and Simple Model Analysis

The first multi-rotational-band structure associated with the wobbling motion have been observed in $^{163}$Lu[1),6)]. The low-spin structure in this nucleus is that of typical well-deformed nucleus; there are many strongly-coupled and aligned rotational bands. At high-spin states, $I \gtrsim 20\hbar$, very regular rotational sequences invade into the yrast region, whose moments of inertia are larger than the usual low-spin bands. These sequences, totally four bands identified in $^{163}$Lu, are believed to be rotational bands based on triaxial and largely deformed configurations, which had been originally speculated by calculations of the potential energy surface more than twenty years ago. Nowadays, similar type of rotational bands are systematically identified in this mass region, Lu and Hf nuclei, and called the triaxial superdeformed (TSD) band. Their triaxiality and deformation are typically $\gamma \approx +20^\circ$ and $\epsilon_2 \approx 0.4$ (in the Lund convention, see Fig. 2), while those of the low-spin normal deformed states are $\gamma \approx 0^\circ$ and $\epsilon_2 \approx 0.2$. The recent experimental progress in $^{163}$Lu is that the interband transitions between TSD1 and TSD2 bands have been observed, where the TSD1 is the yrast TSD band and TSD2 is the first excited (one-phonon) band, and so they indicate clearly the wobbling band structure mentioned in §1. The measured out-of-band transitions is of $I$ to $I-1$, and it has been confirmed to be mainly of E2 character. The $B(E2)$ values[7)] are large and can be nicely reproduced by the simple rotor model. Moreover, the transitions between TSD3 (two-phonon band) and TSD2, and between TSD3 and TSD1 have been also measured

afterward[6]. Quite recently, the same band structure have been observed in neighbouring Lu isotopes, $^{165}$Lu[8] and $^{167}$Lu[9]. In even-even Hf isotopes, $^{168}$Hf[10] and $^{174}$Hf[11], in the same mass region, excited TSD bands have been also measured, although the linking transitions are not measured yet unfortunately.

The interpretation of the observed band structure nicely fits into the prediction first given by Bohr-Mottelson[5] based on the simple rotor model. Let us recall the argument. The rotor hamiltonian is composed of the three body-fixed angular momenta ($J$'s) and three moments of inertia ($\mathcal{J}$'s) around the principal axes in the body-fixed frame:

$$H_{\rm rot} = \frac{J_x^2}{2\mathcal{J}_x} + \frac{J_y^2}{2\mathcal{J}_y} + \frac{J_z^2}{2\mathcal{J}_z} \equiv A_x J_x^2 + A_y J_y^2 + A_z J_z^2. \tag{1}$$

Assuming that $A_x < A_y < A_z$ ($\mathcal{J}_x > \mathcal{J}_y > \mathcal{J}_z$), the yrast state at given angular momentum $I$ is the uniform rotation around the $x$-axis,

$$E_I = \frac{\hbar^2 I^2}{2\mathcal{J}_x}; \quad \langle J_x \rangle \approx \hbar I, \quad \langle J_y \rangle, \langle J_y \rangle \approx \hbar\sqrt{I}. \tag{2}$$

Then the rotational frequency $\omega_{\rm rot}$ is defined, as usual, by $\hbar\omega_{\rm rot} = dE_I/dI$. In the excited state at given $I$ a nucleus rotate non-uniformly around the axis which fluctuates around the main rotation axis ($x$-axis), so that the fluctuating motion of the angular momentum vector is described, in the harmonic approximation, by the following normal mode creation operator:

$$X_{\rm w}^\dagger = a\frac{iJ_y}{\sqrt{2I}} - b\frac{J_z}{\sqrt{2I}}, \quad \text{with} \quad [iJ_y, J_x] = J_x \approx I, \tag{3}$$

where the amplitude $a$ and $b$ satisfy $ab = 1$ due to the normalization condition $[X_{\rm w}, X_{\rm w}^\dagger] = 1$, and they are determined by diagonalizing the rotor hamiltonian (1); $[H_{\rm rot}, X_{\rm w}^\dagger] = \hbar\omega_{\rm w} X_{\rm w}^\dagger$. The explicit calculation leads $\sqrt{2}\,(A_y - A_x)b = \hbar\omega_{\rm w} a/\sqrt{2I}$ and $\sqrt{2}\,(A_z - A_x)a = \hbar\omega_{\rm w} b/\sqrt{2I}$, thus $(\hbar\omega_{\rm w})^2 = 4I(A_y - A_x)(A_z - A_x)$, namely,

$$\hbar\omega_{\rm w} = I\sqrt{(1/\mathcal{J}_y - 1/\mathcal{J}_x)((1/\mathcal{J}_z - 1/\mathcal{J}_x)} = \hbar\omega_{\rm rot}\sqrt{\frac{(\mathcal{J}_x - \mathcal{J}_y)(\mathcal{J}_x - \mathcal{J}_z)}{\mathcal{J}_y\,\mathcal{J}_z}}, \tag{4}$$

where $\omega_{\rm rot} = I/\mathcal{J}_x$ is the rotational frequency of the yrast rotational band. By using this eigen-mode (wobbling mode), the electric E2 transition probabilities of both in-band transitions in the yrast or the one-phonon wobbling bands and out-of-band transitions between them can be also calculated. The basic features are summarized in Fig. 2. As is usual, $B(E2)$ values are sensitive to the deformation, especially in this case to the triaxiality. Here it is to be noted that $0 \le \gamma \le 60^\circ$ is enough for the triaxiality parameter $\gamma$ to specify the shape at zero spin (no rotation). At high-spin states, however, there is an axis of rotation and there are two more regions of triaxial deformation relative to the direction of the rotation axis ($x$-axis). In the figure four possible rotation schemes with axially symmetric deformation are shown, and there are three regions of rotations with triaxial deformation in-between them. As for the E2 transitions from the one-phonon wobbling band to the yrast band, there are two possible transitions, namely from $I$ to $I+1$ or from $I$ to $I-1$. Which transition is stronger is different in each region of triaxiality; the $I$ to $I-1$ transition is stronger in the region 1 and 3, i.e. $0^\circ < \gamma < 60^\circ$ or $-120^\circ < \gamma < -60^\circ$, while the $I$ to $I+1$ transition is stronger in the region 2, i.e. i.e. $-60^\circ < \gamma < 0^\circ$.

Taking into account the basic properties of the wobbling motion in the rotor model, the key quantities are 1) three moments of inertia, $\mathcal{J}_x$, $\mathcal{J}_y$, $\mathcal{J}_z$, and 2) the triaxial deformation, especially the sign of the triaxiality parameter, $\gamma$; both are related in some way. In order for the existence of the wobbling motion, $\mathcal{J}_x$ should be the largest (see Eq. (4)), where $x$-axis is the axis of main rotation of the yrast TSD band. On the other, the $B(E2)$ data suggests positive $\gamma$ shape, $0^\circ < \gamma < 60^\circ$, since only the $I$ to $I-1$ transitions are observed[†], which is also consistent to the calculated position of minimum corresponding to the TSD

[†]The possibility of $-120^\circ < \gamma < -60^\circ$, the region 3 in Fig. 2, cannot be excluded, but it is very unlikely from the spectra of the yrast TSD band.

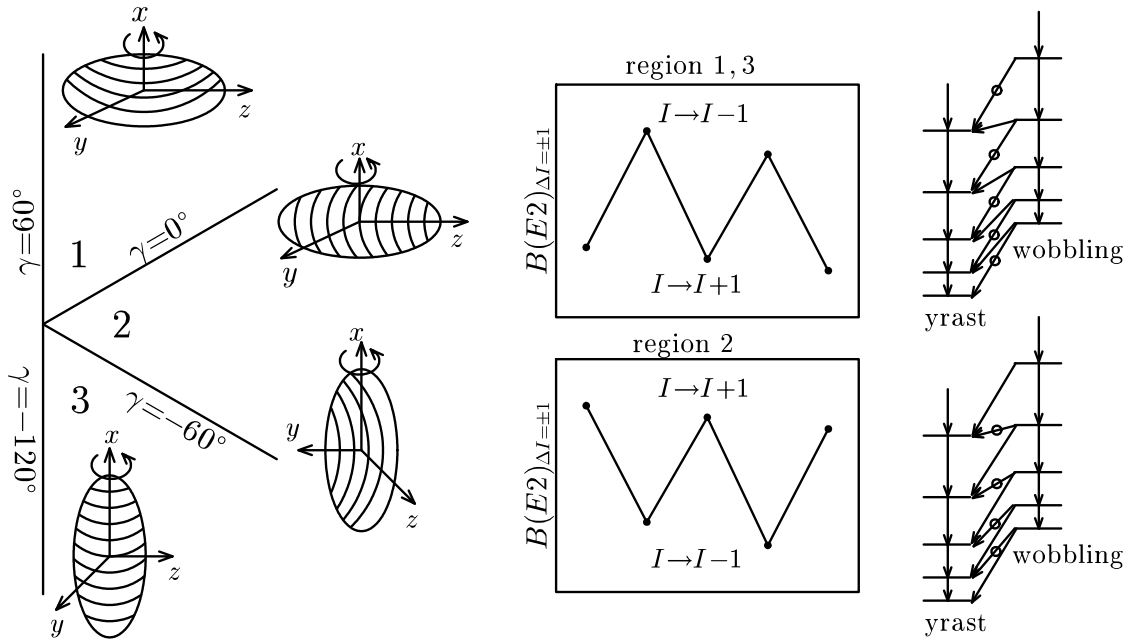


Figure 2: Schematic figure depicting the relation between the triaxial deformation and the properties of the out-of-band E2 transition. The shape corresponding to the triaxiality parameter $\gamma$ (Lund convention) is shown relative to the main rotation axis, which is chosen to the $x$-axis in the left panel. In the middle, the out-of-band $B$(E2) values with $\Delta I = \pm 1$ are plotted as functions of the angular momenta or the rotational frequency, for which stronger transitions are marked in the right panel.

band in the potential energy surface, i.e. $\gamma$(PES) $\approx +20°$. It is, however, stressed that the irrotational moments of inertia, which are commonly used in the rotor model, require $\mathcal{J}_y > \mathcal{J}_x > \mathcal{J}_z$ at positive $\gamma$ ($0° < \gamma < 60°$), and clearly contradict the existence of the wobbling motion ($\hbar\omega_{\rm w}$ in Eq. (4) becomes imaginary). The classical rigid moments of inertia satisfies the condition, in fact $\mathcal{J}_x > \mathcal{J}_y > \mathcal{J}_z$ at positive $\gamma$, but they do not meet the basic quantum mechanics criteria that the rotation should not occur around the symmetry axis, in contrast to the irrotational inertia.

One of the other observed features of the wobbling motion in Lu isotopes is that the wobbling excitation energy $\hbar\omega_{\rm w}$ decreases as a function of the spin $I$ or the rotational frequency $\omega_{\rm rot}$ (see the left panel of Fig. 7 shown later). This trend seems common to all the observed cases in Lu isotopes, but completely opposite to that predicted by the simple rotor model; $\hbar\omega_{\rm w}$ in Eq. (4) is proportional to the rotational frequency if three moments of inertia are assumed to be constant. Therefore, the $\omega_{\rm rot}$-dependence of the wobbling energy requires that three moments of inertia should depend on $\omega_{\rm rot}$ in such a way to decrease $\hbar\omega_{\rm w}$. Another interesting feature to be pointed out is the magnitude of out-of-band $B(E2)_{\rm out}^{I\to I-1}$, which amounts to 100 or more Weisskopf units. Note that the in-band $B(E2)_{\rm in}^{I\to I-2}$ value is larger and about 500 or more Weisskopf units in TSD bands, which are consistent with the calculated deformation parameters ($\epsilon_2 \approx 0.4, \gamma \approx +20°$) by the potential energy surface, and so the out-of-band transitions is about 20% of the in-band transitions. These transitions are extremely strong and suggests that both are of rotational origin, which are nicely reproduced by the simple rotor model. As examples of strong out-of-band E2 transitions, those between the ground state band and the collective $\beta$- or $\gamma$-vibrational band are known in well-deformed nuclei. Their $B(E2)$ values are typically about 5 – 8 Weisskopf units, while the typical in-band E2 transition probabilities of normal deformed nuclei are 100 – 200 Weisskopf units.

In the Lu isotopes the odd proton particle exists in addition to the simple rotor. Therefore one has to consider the more elaborated particle-rotor coupling model[12]. The essential features discussed above are not changed as long as three moments of inertia satisfying $\mathcal{J}_x > \mathcal{J}_y > \mathcal{J}_z$ are used, although the presence of the odd particle makes the rotational spectra more complex.

## 3 Microscopic RPA Model

Considering the observed features of the wobbling motion discussed in the previous section, the simple rotor model fails; namely one cannot use the irrotational moments of inertia and the dependence of three moments of inertia on the rotational frequency should be taken into account. Since we do not know what kind of moments of inertia should be used *a priori*, we have to calculate three moments of inertia, which requires a microscopic framework to study the wobbling motions. Such a framework were proposed by Marshalek[13], and examined in details in some realistic cases in Ref. 14).

The theory is based on the random phase approximation (RPA) on top of the cranked mean-field, which is used to describe the uniform rotation of the yrast (vacuum) rotational band by the stationary mean-field hamiltonian, $h' = h_{\rm def} - \omega_{\rm rot} J_x$. In the one-phonon wobbling band the fluctuating motion is not so large, and the small amplitude approximation of time-dependent mean-field around $h'$ can be used, which results in the RPA eigen-mode equation. Thus, with using the $QQ$ type force as a residual interaction, the $n$-th eigen-energy $\hbar\omega_n$ and eigen-mode creation operator $X_n^\dagger = \sum_{\alpha\beta}\left[\psi(\alpha\beta)a_\alpha^\dagger a_\beta^\dagger - \phi(\alpha\beta)a_\beta a_\alpha\right]$ as a superposition of two-quasiparticle excitations can be calculated. If the $n$-th mode is identified as a wobbling motion, $X_n^\dagger$ and $\hbar\omega_n$ correspond to $X_{\rm w}^\dagger$ and $\hbar\omega_{\rm w}$ in Eqs. (3), (4) in the simple rotor model. The $QQ$ type force contains the quadrupole tensor, $Q_{ij} = \sqrt{\frac{15}{4\pi}}\sum_{a=1}^{A}\left[x_i x_j - \frac{1}{3}r^2\delta_{ij}\right]_a$ ($i,j = x,y,z$, in the Cartesian representation), but, because of the symmetry such that the wobbling excitation changes the angular momentum by $\pm 1$ unit, only the two components, $Q_y \equiv -Q_{zx}$ and $Q_z \equiv i\,Q_{xy}$ are responsible for dynamical time-dependence[†]. Thus the time-dependent mean-field is

$$h_{\rm UR}(t) = h_{\rm def} - \omega_{\rm rot}J_x - \kappa_y \mathcal{Q}_y(t)Q_y - \kappa_z \mathcal{Q}_z(t)Q_z, \tag{5}$$

where $\kappa_{y,z}$ are the $QQ$ type force strengths, and $\mathcal{Q}_{y,z}(t) = \langle t|Q_{y,z}|t\rangle$ describe the time-dependence of the relevant quadrupole components. The subscript UR is attached because this time-dependent hamiltonian is defined in the uniformly rotating (UR) frame, where the rotation axis is pointing to the main rotation axis ($x$-axis) of the vacuum band. The wobbling excitation on it induces the shape fluctuation of the non-diagonal quadrupole tensor, $\mathcal{Q}_y(t)$ and $\mathcal{Q}_z(t)$, in the mean-field, and the out-of-band E2 transition probabilities are calculated by

$$B(E2)_{\rm out}^{I\to I\mp 1} = \tfrac{1}{2}|\mathcal{Q}_y^{(E)}(n) \pm \mathcal{Q}_z^{(E)}(n)|^2, \tag{6}$$

where $\mathcal{Q}_{y,z}^{(E)}(n)$ are the electric (proton) part of tensor calculated with only the $n$-th eigen-mode being excited. In order to recover the wobbling picture of the angular momentum fluctuation, the time-dependent non-unitary transformation to the principal axis (PA) frame should be performed by requiring that the non-diagonal part of quadrupole tensor should vanish. Then the time-dependent mean-field in the PA frame is now

$$h_{\rm PA}(t) = h_{\rm def} - \omega_x(t)J_x - \omega_y(t)J_y - \omega_z(t)J_z, \tag{7}$$

where $\omega_x(t) \approx \omega_{\rm rot}$ in the small amplitude limit, and $\omega_{y,z}(t)$ being related to $\mathcal{Q}_{y,z}(t)$ describe the fluctuation of the angular frequency vector. In this frame, the fluctuation of the angular momentum vector naturally arises, $\langle t|J_{y,z}|t\rangle$: Then the three RPA moments of inertia are introduced through

$$\mathcal{J}_x \equiv \langle J_x\rangle/\omega_{\rm rot}, \quad \mathcal{J}_{y,z}(n) \equiv J_{y,z}(n)/\omega_{y,z}(n), \tag{8}$$

where the frequencies $\omega_{y,z}(n)$ and the expectation values $J_{y,z}(n)$ are calculated with only the $n$-th eigen-mode being excited. What Marshalek found is that using these three moments of inertia the RPA phonon energy can be expressed in the same way as in Eq. (4) in the simple rotor model, namely the wobbling energy equation is equivalent to the RPA eigen-mode equation. The dynamical pictures of the wobbling motion in the UR and PA frames are shown schematically in Fig. 3.

[†]If is used the usual spherical tensor representation with classification by the signature quantum number, $Q_{2K}^{(\pm)}$, then $Q_y = Q_{21}^{(-)}$ and $Q_z = Q_{22}^{(-)}$, i.e. they transfer signature by one unit.

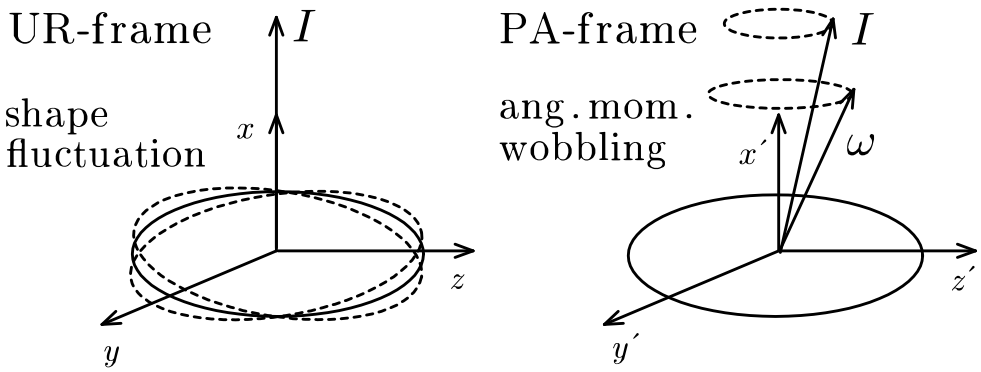


Figure 3: Schematic figure depicting the two dynamical pictures in the uniformly rotating frame (UR frame) and the principal axis frame (PA frame).

In this way, the wobbling phonon energy, the $B(E2)$ values, and the three moments of inertia can be calculated in a microscopic framework without ambiguity. We would like to stress that the $QQ$ type force strengths $\kappa_{y,z}$ in Eq. (5) are not free parameters but fixed by the requirement of the decoupling of the Nambu-Goldstone modes in the RPA. Therefore, there is no adjustable parameters once the mean-field parameters are fixed selfconsistently. It should also be noticed that the number of RPA eigen-modes are that of independent two-quasiparticle states, but most of the solutions do not have a proper wobbling property. For example, the defined $\mathcal{J}_{y,z}(n)$ can take negative values, or the fluctuation amplitude of the angular momentum vector is too small if the obtained E2 amplitudes $\mathcal{Q}_y(n)$ and $\mathcal{Q}_z(n)$ are not collective; such solutions are not wobbling mode at all. In fact, the RPA solution which can be interpreted as a wobbling motion do not always appear: Some condition on the mean-field is necessary.

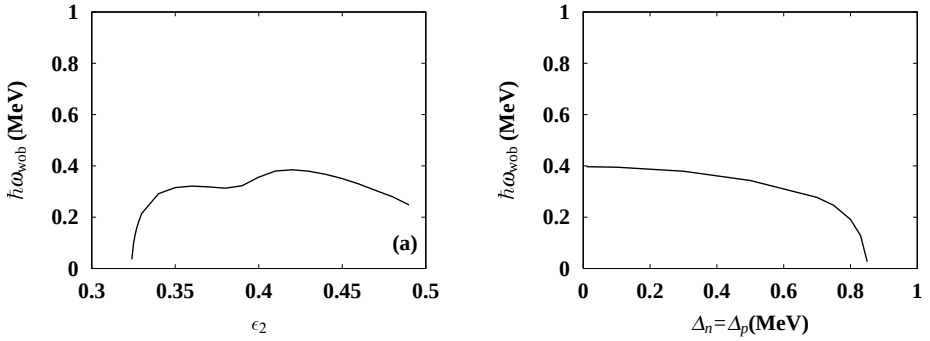


Figure 4: Wobbling excitation energy calculated as a function of the deformation parameter $\epsilon_2$ (left), and of the static pairing gap parameter $\Delta_{\rm n,p}$ (right), in an even-even nucleus $^{168}$Hf. Taken from Ref. 16).

In Figs. 4 and 5 we show an example depicting the dependences of the wobbling energy $\hbar\omega_{\rm w}$ on various mean-field parameters, $\epsilon_2$, $\gamma$ and pairing gap $\Delta_{\rm n,p}$ calculated at $\hbar\omega_{\rm rot} = 0.3$ MeV in a even-even nucleus $^{168}$Hf. The collective wobbling solution indeed exists around the expected values of parameters $\epsilon_2 \approx 0.4$ and $\gamma \approx +20°$, and it is stable against the change of the pairing gap parameters, which are supposed to be small ($\Delta \lesssim 0.5$ MeV) in the TSD bands. It should be noted that the wobbling mode becomes softer ($\hbar\omega_{\rm w}$ decreases) as $\Delta$ increases, which is opposite behaviour to the case of the conventional collective vibrational modes, and may indicate that it is of rotational character. The three RPA moments of inertia are also shown in Fig. 5, from which it is clear that they are neither irrotational nor rigid-body like. We further show the wobbling energy and RPA moments of inertia as functions of the rotational frequency $\omega_{\rm rot}$ in Fig. 6; unfortunately the wobbling motion is not established yet in this nucleus. Here the mean-field parameters are fixed for simplicity; $\epsilon_2 = 0.43$, $\gamma = +20°$, and $\Delta_{\rm n} = \Delta_{\rm p} = 0.3$ MeV. In the

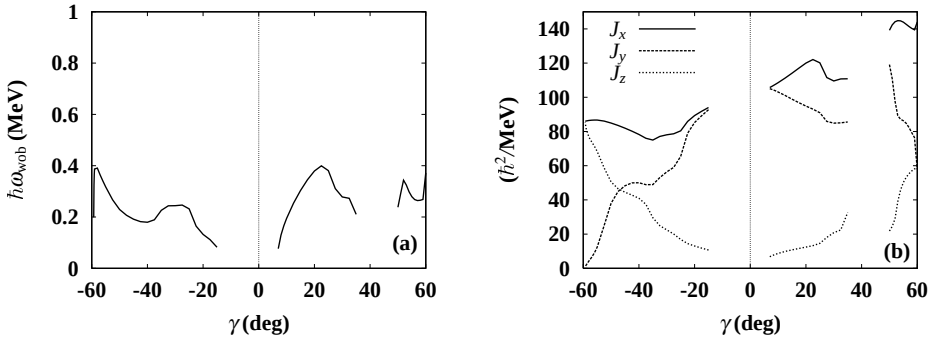


Figure 5: Wobbling excitation energy (left) and three moments of inertia (right) as functions of the triaxiality parameter $\gamma$, in an even-even nucleus $^{168}$Hf. Taken from Ref. 16).

microscopic RPA calculation the $\omega_{\rm rot}$-dependence naturally arises as a result of cranking prescription of the quasiparticle orbits, and the wobbling energy is not simply proportional to the rotational frequency.

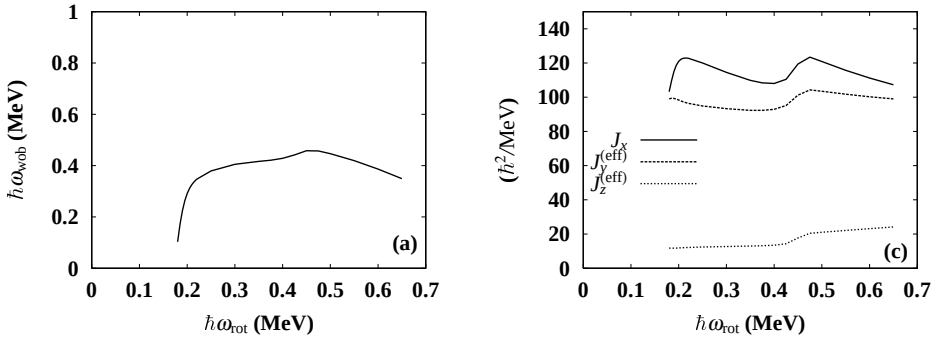


Figure 6: Wobbling excitation energy (left) and three RPA moments of inertia (right) as functions of the rotational frequency $\omega_{\rm rot}$, in an even-even nucleus $^{168}$Hf. Taken from Ref. 16).

It is known that the microscopically calculated $\gamma$-dependence of three moments of inertia at zero rotational frequency, e.g. by the Inglis cranking formula, look very similar to the irrotational inertia. If that is the case, why does the wobbling solution appear in our microscopic RPA calculations? The reason is the following: The $\mathcal{J}_x$ inertia in the RPA formalism in Eq. (8) is that of kinematic moment of inertia, so that the alignments of quasiparticle orbits contribute to it. Actually the occupation of the high-$j$ proton $i_{13/2}$ quasiparticle is essential to generate a minimum at the positive $\gamma$ shape for the TSD bands. As is seen in Fig. 6, the alignment of two $\pi i_{13/2}$ quasiparticles occurs around $\hbar\omega_{\rm rot} \approx 0.2$ MeV, which suddenly increases $\mathcal{J}_x$. Because of this effect the condition $\mathcal{J}_x > \mathcal{J}_y(n) > \mathcal{J}_z(n)$ is satisfied and the wobbling solution appears. Thus the increase of $\mathcal{J}_x$ due to the quasiparticle alignments is crucial for the appearance of the wobbling motion in our RPA calculations; see Ref. 15) and 16) for details.

Now we compare the calculated results with experimental data for $^{163}$Lu in Fig. 7, where, again, all the mean-field parameters are fixed. The calculated wobbling energy $\hbar\omega_{\rm w}$ is smaller than the experimental data and stays almost constant against the rotational frequency $\omega_{\rm rot}$, while, as already mentioned, the experimental wobbling energy decreases with $\omega_{\rm rot}$. Thus, the result of calculation is not very successful to reproduce the detailed $\omega_{\rm rot}$-dependence. This requires that the change of the mean-field parameters as functions of $\omega_{\rm rot}$ should be considered. Even more problematic is the out-of-band $B(E2)$ values, which are about 2–3 times smaller than the experimentally measured values. Here we would like to recall that the measured $B(E2)$ is very large, more than 100 Weisskopf units: Although the calculated $B(E2)$ values are extremely large compare to those in the case of usual collective vibrations, it is not enough to reproduce those of the wobbling mode. Considering the sum-rule like argument in Ref. 16), we feel it is very difficult

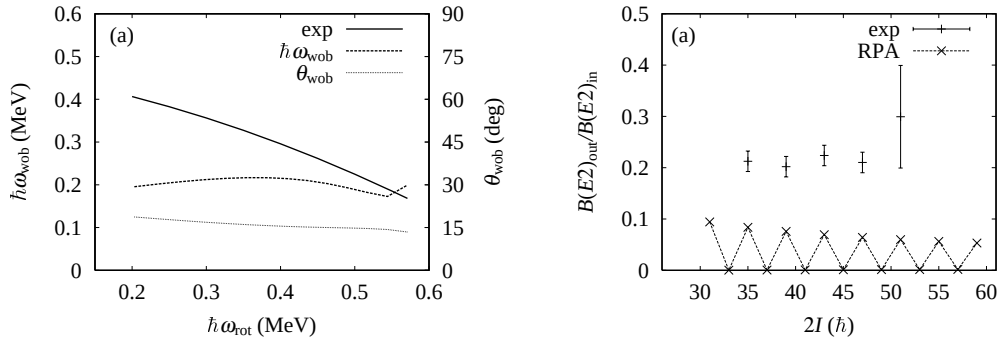


Figure 7: Comparison of the calculated wobbling energy (left) and the $B(E2)$ value (right) with experimental data in $^{163}$Lu nucleus. In the left panel, the wobbling amplitude $\theta_{\rm w} \equiv \tan^{-1}(\sqrt{J_y(n)^2 + J_z(n)^2}/\langle J_x \rangle)$ is also shown, see Ref. 15) for details.

for the microscopic RPA theory to understand that the macroscopic rotor limit of the out-of-band $B(E2)$ value is almost reached in the actual nucleus.

# 4 Summary and Discussions

In this talk, recently identified nuclear wobbling motions in the Lu and Hf region are reviewed and discussed from the microscopic view point. The original picture of the wobbling motion is based on the simple rotor model. It is, however, apparent that the atomic nucleus is not macroscopic object like a rotor. Therefore, the observed properties of the wobbling motion cannot be always understood by the rotor model, and one has to invoke more fundamental microscopic theories. We summarize the points of our investigations up to now, which have been done by means of the microscopic RPA framework in the previous section, as follows:

(1) By suitable choice of the mean-field parameters, i.e. large enough $\epsilon_2$ and positive $\gamma \approx +20^\circ$, we have found that low-energy wobbling solutions appear naturally among the RPA eigen-modes. The wobbling solution is insensitive to the pairing gap parameters; the eigen-energy decreases as the gap increases, which is a completely opposite behaviour compared with the case of low-lying collective vibrations.

(2) The proton $i_{13/2}$ quasiparticle alignments are crucial to obtain the condition $\mathcal{J}_x > \mathcal{J}_y(n) > \mathcal{J}_z(n)$ for the RPA moments of inertia, which is required for the existence of the associated wobbling mode. It is consistent with the fact that the occupation of the same proton $i_{13/2}$ quasiparticle is necessary for the positive $\gamma$ TSD shape to be minimum in the potential energy surface calculations.

(3) The detailed rotational frequency dependence of the wobbling excitation energy could not be reproduced in the present RPA calculation, although it is much improved compared with the result of the simple rotor model with fixed moments of inertia, which gives completely opposite dependence to the experimental data. All the mean-field parameters are assumed to be constant for simplicity in our calculations. This result suggests that change of the mean-field against the rotational frequency should be properly taken into account.

(4) A severe problem of the RPA calculations is that the out-of-band $B(E2)$ values are smaller by about factor two or three than the experimentally measured values. Although the obtained RPA solution is extremely collective, the collectivity (enhancement of $B(E2)$) is not enough. This poses an important future challenge for the microscopic theory like RPA.

Finally we would like to discuss a possible explanation of the calculated dependence of the wobbling energy $\hbar\omega_{\rm w}$ on the rotational frequency $\omega_{\rm rot}$ (or spin $I$), i.e. increasing in the lower frequency and decreasing in the higher frequency, which are shown in Figs. 6 and 7 (see Ref. 16) for more examples of calculation). It is based on a rotor model with a modification to include the effect of quasiparticle alignments, which is investigated in Ref. 12), but the possibility is not thoroughly explored[†]. The hamiltonian is the same as Eq. (1) except that the $J_x$ is now replaced to $(J_x - j)$, where $j$ is a constant and corresponds to the aligned angular momentum of quasiparticle(s). Expanding the $(J_x - j)^2$ term, a linear term $-jJ_x/\mathcal{J}_x$ in $J_x$ appears. Treating this term by $J_x = \left[I^2 - (J_y^2 + J_z^2)\right]^{\frac{1}{2}} \approx I - (J_y^2 + J_z^2)/2I$ in the high-spin limit, the modified rotor hamiltonian and the yrast energy are given by

$$\tilde{H}_{\rm rot} \approx \frac{J_x^2}{2\mathcal{J}_x} + \frac{J_y^2}{2\tilde{\mathcal{J}}_y(I)} + \frac{J_z^2}{2\tilde{\mathcal{J}}_z(I)} + \left(\frac{j^2 - 2Ij}{2\mathcal{J}_x}\right), \quad E_I = \frac{(I-j)^2}{2\mathcal{J}_x}, \tag{9}$$

and the rotational frequency is now given by $\hbar\omega_{\rm rot} = (I-j)/\mathcal{J}_x$. The last term in $\tilde{H}_{\rm rot}$ is constant, and

$$\tilde{\mathcal{J}}_{y,z}(I) = \mathcal{J}_{y,z}\left[1 + \frac{j\mathcal{J}_{y,z}}{I\mathcal{J}_x}\right]^{-1} \tag{10}$$

are the modified $I$-dependent moments of inertia. Namely, the effect of the quasiparticle alignments makes $\tilde{\mathcal{J}}_{y,z}(I)$ inertia smaller. Since the diagonalization of Eq. (9) in terms of the wobbling mode (3) is the same if $\mathcal{J}_{y,z}$ are replaced by $\tilde{\mathcal{J}}_{y,z}(I)$, the wobbling mode appears in the spin range, $j < I < I_{\rm crit} \equiv j[1 - \mathcal{J}_x/\mathcal{J}_y]^{-1}$, because the condition $\mathcal{J}_x > \tilde{\mathcal{J}}_y(I) > \tilde{\mathcal{J}}_z(I)$ is satisfied in $I < I_{\rm crit}$ ($j < I$ is required for $\hbar\omega_{\rm rot} = dE_I/dI > 0$), even when the original three inertia are $\mathcal{J}_y > \mathcal{J}_x > \mathcal{J}_z$ like the irrotational inertia at the positive $\gamma$ shape. An example of the wobbling excitation energy calculated with this modified $\tilde{H}_{\rm rot}$ is shown in Fig. 8. Even though the original three inertia are constants, a similar $\omega_{\rm rot}$-dependence to those in the realistic RPA calculations emerges because of the presence of the quasiparticle alignments. It is, however, mentioned that the appearance mechanism of the wobbling motion is somewhat different from the interpretation of the RPA calculation given in §3: $\mathcal{J}_x$ is increased by the alignments in the RPA, while $\mathcal{J}_{y,z}$ are decreased in this modified rotor model, although the quasiparticle alignments play an essential role in both explanations. At this stage we are not sure that this model serves as a possible model explaining the results of the microscopic RPA calculations. But we hope that this kind of interpretation of the calculated results by an intuitive model deepens insight into the appearance mechanism of the wobbling motion, and gives some clues for improving the microscopic framework.

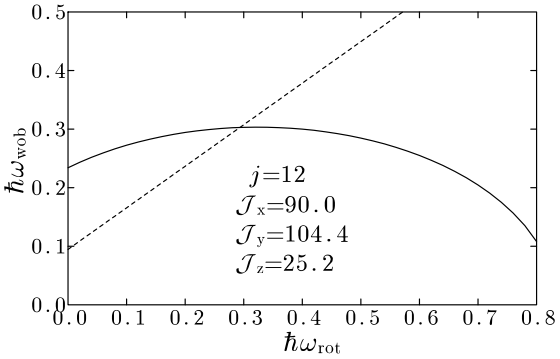


Figure 8: An example of the wobbling excitation energy in the modified rotor hamiltonian (9) as a function of $\hbar\omega_{\rm rot} = (I-j)/\mathcal{J}_x$. The (rather arbitrarily) chosen values of the quasiparticle alignment $j$ and three inertia $\mathcal{J}_y > \mathcal{J}_x > \mathcal{J}_z$ are shown in the figure. The dashed line is the original wobbling energy (4) calculated by replacing $\mathcal{J}_x$ and $\mathcal{J}_y$ (so-called $\gamma$-reversed inertia[12)]).

[†]The following argument results from the discussion with Stefan Frauendorf.

## Acknowledgments

Discussion with Stefan Frauendorf at ECT* in Trento is greatly appreciated. This work was supported in part by the Grant-in-Aid for scientific research from the Japan Ministry of Education, Science and Culture (Grant Nos. 13640281 and 14540269).

## References

1) S. W. Ødegård et al., Phys. Rev. Lett. **85** (2001), 5866; D. R. Jensen et al., Nucl. Phys. **A703** (2002), 2.
2) S. Frauendorf, Rev. Mod. Phys. **73** (2001), 463.
3) S. Frauendorf and J. Meng, Nucl. Phys. **A617** (1997), 131.
4) K. Starosta, et al., Phys. Rev. Lett. **86** (2001), 971; T. Koike, et al., Phys. Rev. **C67** (2003), 044319.
5) A. Bohr and B. R. Mottelson, *Nuclear Structure*, Vol. II, Benjamin, New York, 1975.
6) D. R. Jensen et al., Phys. Rev. Lett. **89** (2002), 140523; D. R. Jensen et al., Eur. Phys. J. **A19** (2004), 173.
7) A. Gögen, et al., Phys. Rev. **C69** (2004), 031301(R).
8) G. Schönwaßer, et al., Phys. Lett. **B552** (2003), 9.
9) H. Amro, et al., Phys. Lett. **B553** (2003), 197.
10) H. Amro, et al., Phys. Lett. **B506** (2001), 39.
11) M. K. Djongolov, et al., Phys. Lett. **B560** (2003), 24.
12) I. Hamamoto, Phys. Rev. **C65** (2002), 044305; I. Hamamoto and G. B. Hageman, Phys. Rev. **C67** (2003), 014319.
13) E. Marshalek, Nucl. Phys. **A331** (1979), 429.
14) M. Matsuzaki, Nucl. Phys. **A509** (1990), 269; Y. R. Shimizu and M. Matsuzaki, Nucl. Phys. **A588** (1995), 559.
15) M. Matsuzaki, Y. R. Shimizu, and K. Matsuyanagi, Phys. Rev. **C65** (2002), 041303(R).
16) M. Matsuzaki, Y. R. Shimizu, and K. Matsuyanagi, Phys. Rev. **C69** (2004), 034325.